Life Sciences 235 (2019) 116842

Contents lists available at ScienceDirect

Life Sciences

journal homepage: www.elsevier.com/locate/lifescie

Antagonism of miR-429 ameliorates anoxia/reoxygenation injury in cardiomyocytes by enhancing MO25/LKB1/AMPK mediated autophagy

Qingqing Zhu[a,*], Fangfang Hu[b]

[a] The First Ward, Department of Cardiology, Huaihe Hospital of Henan University, Kaifeng 475000, China
[b] The Third Ward, Department of General Surgery, Huaihe Hospital of Henan University, Kaifeng 475000, China

ARTICLE INFO

Keywords:
miR-429
MO25
Cardiomyocytes
MO25/LKB1/AMPK
Autophagy

ABSTRACT

MicroRNAs plays important role in the development of myocardial infarction (MI). The aim of this study was to analyze whether miR-429 has effect on the process of autophagy in myocardial anoxia/reoxygenation (AR) or ischemia/reperfusion (IR) injury and explore the underlying mechanism. The results showed that miR-429 was significantly decreased in MI mouse hearts and AR treated cardiomyocytes. Dual luciferase activity assay proved that MO25 was the direct target of miR-429. MO25 was dramatically decreased in AR treated cardiomyocytes. Overexpression of miR-429 dramatically decreased the expression of MO25, whereas inhibition of miR-429 noticeably increased the expression of MO25. In addition, overexpression of miR-429 reduced GFP-LC3B labelled cells, decreased the number of vesicle and autophagosome in each cardiomyocyte, and induced cell apoptosis in AR treated cardiomyocytes. In contrast, inhibition of miR-429 had the opposite effect. The further *in vivo* study showed that when mouse in IR group were injected with antagomiR-429, the weight of left ventricular was increased and infarct size was significantly decreased. Finally, both the *in vitro* and *in vivo* study showed that the expression of MO25, LKB1, pAMPKa, ATG13, p62 and LC3BI/II was noticeably increased by antagomiR-429. In conclusion, our results suggested that antagonism of miR-429 ameliorates anoxia/reoxygenation injury in cardiomyocytes by enhancing MO25/LKB1/AMPK mediated autophagy.

1. Introduction

Myocardial infarction (MI) is a major cause of death and disability worldwide in patients with coronary heart disease [1]. MI represents an enormous clinical challenge as loss of myocardium [2]. Although much advances has been achieved in the diagnosis, treatment, and prognosis of MI, MI is still reported to be a single largest cause of death in the United states, responsible for 1 out of every 6 deaths [3]; and it is estimate that 16 million people will suffer acute MI in 2020 and 23 million in 2030 in China [4]. Therefore, an early detection and correct diagnosis of MI are urgent to seek to prevent the progressive development of MI, and reduce the mortality rate in patients.

It is reported that anoxia/reoxygenation (AR) injury is involved in the progression of MI, and can induce the altered expression of miRNAs (miRNAs) [5]. MiRNAs are a class of non-coding single stranded small RNA consisting of 21-23nucleotides, are negative regulators of gene expression by binding to 3′UTR of mRNA [6]. MiRNAs act as essential modulators in various biological processes, such as cell proliferation [7], apoptosis [8], angiogenesis [9], autophagy [10], et al. Mounting evidences show that miRNAs also play an important role in the progression of MI, such as miR-221-3p [11], miR-181a [12], miR-103a [13], et al. Previous study showed that down-regulation of miR-429 protected cardiomyocytes against hypoxia-induced apoptosis [14], whereas the effect miR-429 on the progression of autophagy in MI still remains unknown. So, this study aims to analyze whether miR-429 has effect on the process of autophagy in MI and explore the underlying mechanism.

2. Materials and methods

2.1. The mouse model of ischemia/reperfusion (IR) injury

C57BL/6 mice (20–25 g, 10 weeks) were obtained from BetterBiotechnology Co., Ltd. (Nanjing, China). All animal studies were conducted accordance with the institutional Guideline for Animal Research and the Guide for the Care and use of Laboratory Animals published by the National Institutes of Health (NIH Publication, 8th Edition, 2011). First, the mice were anesthetized by intraperitoneal injection with xylazine (5 mg/kg) and ketamine (100 mg/kg). Then, the left coronary artery (LCA) permanent ligation for 45 min, and the next

* Corresponding author at: The First Ward, Department of Cardiology, Huaihe Hospital of Henan University, Baobei Road No.8, Kaifeng 475000, China.
E-mail address: qingqingzhuhhyy@163.com (Q. Zhu).

https://doi.org/10.1016/j.lfs.2019.116842
Received 6 June 2019; Received in revised form 4 September 2019; Accepted 4 September 2019
Available online 05 September 2019
0024-3205/

24 h of reperfusion was conducted according to previous study described [15]. Myocardial blanching and continuous electrocardiography monitoring showing ST segment elevation was used to confirm ischemia. Finally, the mice were euthanasia. To investigate the effect of miR-429 on the mice model of IR, antagomiR-429 or the control antagomiR was injected into the left ventricular free wall using a syringe with a 30-gauge needle before IR model was build. After the treatment, the weight of left ventricular was measured. The infarct size was measured by TTC staining.

2.2. Primary cardiomyocytes culture and anoxia/reoxygenation treatment

The Sprague-Dawley neonatal rats (2-day old) were obtained from Better Biotechnology Co., Ltd. (Nanjing, China). The cardiomyocytes were isolated from neonatal rat hearts and cultured in DEME supplemented with 20% FBS according to previous study described [16]. To establish AR injury model, cardiomyocytes were subjected to hypoxia (94% N_2, 5% CO_2, 1% O_2) for 3, 6 and 12 h. After anoxia, cardiomyocytes were exposed for 2 h of reoxygenation under normal condition. The control group cells were maintained at normoxia for the same duration.

2.3. Transfection

MiR-429 mimic, antagomiR-429 and the corresponding controls were obtained from GenePharma (Shanghai, China). Before cardiomyocytes were under the treatment of AR, the cells were transfected with miR-429 mimic, antagomiR-429 and the corresponding controls using Lipofectamine 2000 reagent (Invitrogen, Carlsbad, CA, USA).

2.4. Real time PCR

After the mouse model of MI were successfully build for 1 d, 1 week, 2 weeks and 4 weeks, or the AR injury model were successfully build at different time, the total RNA of heart tissues or cells were isolated using TRIzol® Reagent (Thermo Fisher Scientific, Waltham, MA). The first strand DNA was synthesized using the PrimeScript RT reagent kit (TakaRa, Dalian, China). The Real-time PCR was performed according to the instruction of SYBR Premix Ex Taq II (TaKaRa) kit. The reaction was run in ABI7500 Real-time PCR system (Applied Biosystems, Carlsbad, CA). The reaction program was as follows: 95 °C for 5 min for initial degeneration, and followed by 40 cycles at 95 °C for 10 s and 60 °C for 34 s. All primers used in this study were synthesized from Sangon Biotech (Shanghai, China). The relative expression of gene were quantified with $2^{-\triangle\triangle CT}$ method.

2.5. Western blot

The heart tissues or cardiomyocytes were lysed using RIPA lysis buffer (Thermo Fisher) and the protein concentration was measured using BCA Protein Kit (Thermo Fisher). The protein (20 μg) was separated on 10% SDS-PAGE and then transferred to polyvinylidene fluoride (PVDF) membranes. The blots were probed with rabbit anti-p62 (Abcam, Cambridge, UK; 1: 500 dilution), rabbit anti-LC3B (Abcam, 1: 2000 dilution), rabbit anti-MO25 (Abcam, 1: 20000 dilution), rabbit anti-LKB1 (Abcam,1: 1000 dilution), rabbit anti-pAMPKa (Cell Signalling Technology, Beverly, MA, USA), rabbit anti-ATG13 (Abcam, 1: 1000 dilution) for overnight at 4 °C. The blots were incubated with horse radish peroxide-conjugated secondary antibody. The imaging was performed with Enhanced Chemiluminescent Kit User Manual according to the instruction. Finally, the proteins were visualized with an Anmobilon Western Chemiluminescent HRP Substrate system (Millipore Corp., Billerica, MA, USA).

2.6. Dual luciferase activity assay

HEK 293 cells were co-transfected with miR-429 mimic and p-MIR-report plasmid (Ambion, Austin, TX, USA) containing the wide type of 3′-UTR of MO25, or co-transfected with miR-324-5p mimic and p-MIR-report plasmid (Ambion, Austin, TX, USA) containing the mutant type of 3′-UTR of MO25, or transfected with mimic control and p-MIR-report plasmid (Ambion, Austin, TX, USA) containing the 3′-UTR of MO25. The control group was transfect with only p-MIR-report plasmid. Luciferase activity was measured using a dual-luciferase reporter assay system (Promega, WI, USA) after 48 h of transfection.

2.7. GFP-LC3B puncta

Adenoviral GFP-LC3B was purchased from ThermoFisher. Adenoviral GFP-LC3B was used to detect autophagosome formation in cardiomyocytes that transfected with miR-429 mimic, antagomiR-429 or their relative control, and exposed to A6h/R2h. Cells were fixed and imaged for autophagic puncta detection using a Nikon TE300 fluorescence microscope. Images were deconvolved using Autodeblur Software and formatted with ImageJ. Once the number of autophagic puncta reached 20, the cells were regarded as positive for autophagy.

2.8. Electron microscopic examination

The number of vesicle and autophagosome in each cardiomyocytes was examined by electron microscopic.

2.9. TUNEL assay

Cell apoptosis was measured by TUNEL staining. The cells cultured on coverslips in 6-well plates were fixed in 4% paraformaldehyde. The TUNEL staining was performed using the *in situ* cell death detection kit (Minneapolis, MN, USA) according to the instruction. The number of TUNEL-positive cells and the total cells were counted under a fluorescence microscope.

2.10. Echocardiography

For echocardiography analysis, mice chests were shaved and allowed to rest by at least 1 h before echocardiography, which was performed on conscious mice to avoid any cardio depression produced by anesthesia. Mice were ascertained using the M mode short axis view, measuring systolic and diastolic cardiac dimensions by using the BL-420S Biology Function Laboratory System (Techman Soft, Chengdu, China).

2.11. Statistical analysis

All the data were analyzed using SPSS 19.0 software. Data were presented in the form of mean ± standard deviation (SD). The independent student's *t*-test was applied to compare the quantitative parameters between two groups. Analysis of Variance (ANOVA) was used to compare several groups. A value of $P < 0.05$ was considered of significance.

3. Results

3.1. MiR-429 was significantly down-regulated in IR mouse and AR treated-cardiomyocytes

In order to analyze the effect of miR-429 on the process of autophagy in MI, we first measured the expression of miR-429 in mice model of MI. The results of Real-time PCR showed that the miR-429 was significantly down-regulated in mouse model of MI from week 1 to the end of week 4 (Fig. 1A, $P < 0.05$) compared with sham group. Further, we

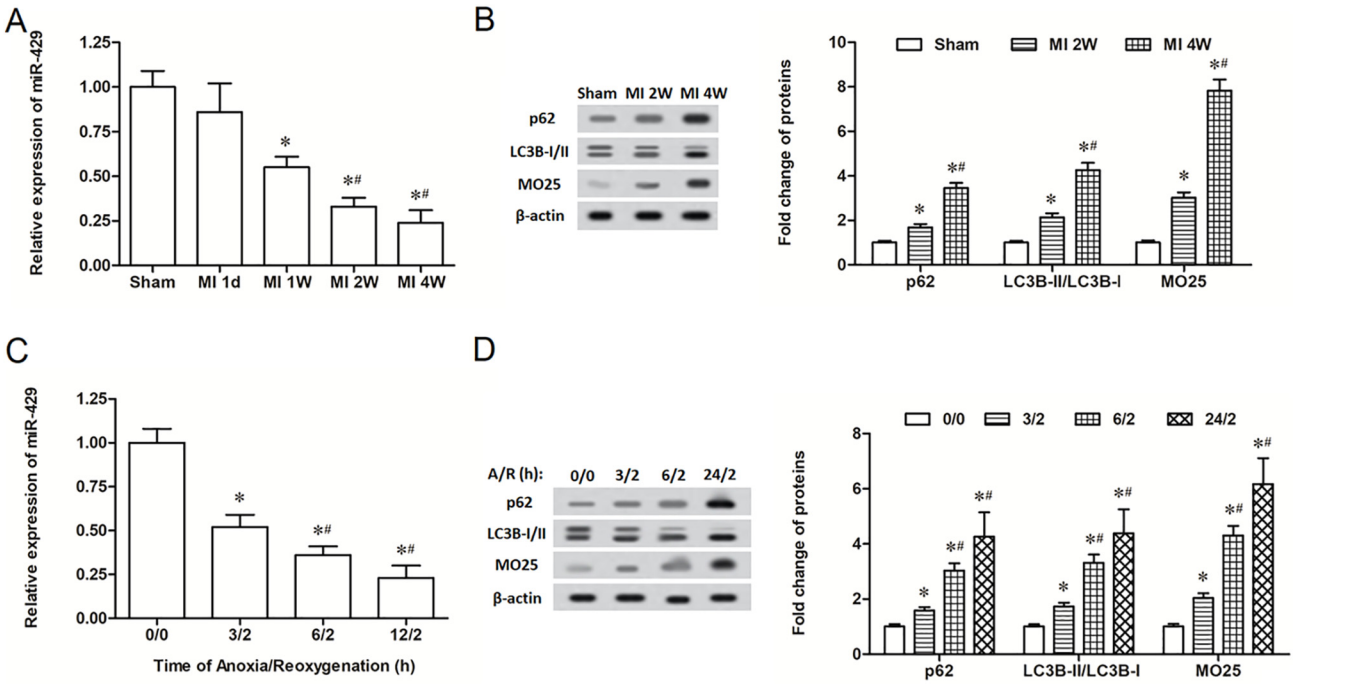

Fig. 1. MiR-429 was significantly down-regulated in IR mouse and anoxia/reoxygenation cells. A. After the IR mouse model was successfully build for 1 d, 1 w, 2 w and 4 w, the heart tissues were isolated and the expression of miR-429 was measured by Real-time PCR. B. The expression of p62, LC3BI/II of heart tissues was measured by Western blot. C. After the cardiomyocytes were treated with anoxia for 3, 6 and 12 h, followed by 2 h reoxygenation, the expression of miR-429 was measured by Real-time PCR. D. B. The expression of p62, LC3BI/II in cardiomyocytes was measured by Western blot. $^{*}P < 0.05$ *vs* Sham or 0/0; $^{\#}P < 0.05$ *vs* MI 1 W or 3/2.

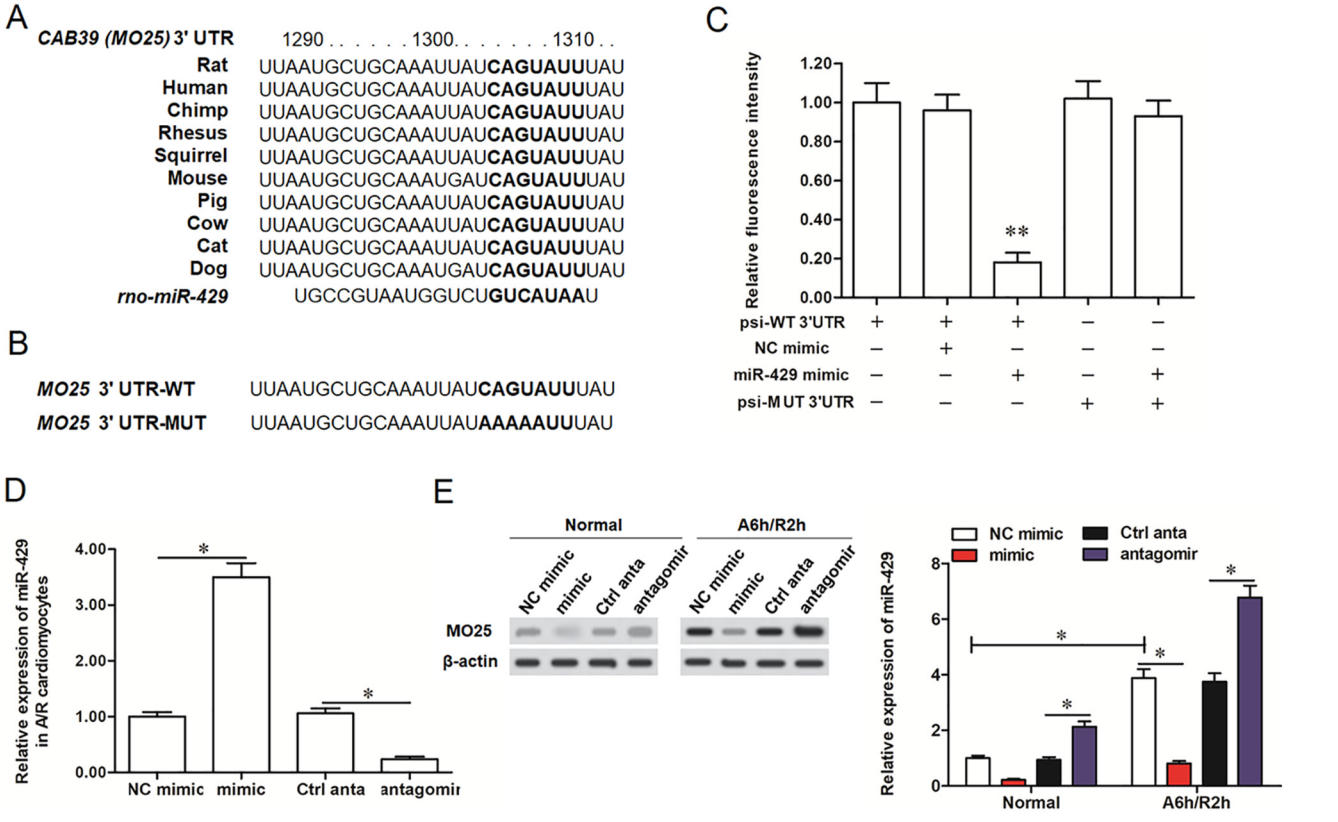

Fig. 2. MO25 was the direct target gene of miR-429. A. Sequence of alignment of putative miR-429 binding site in 3′UTR of MO25 of several species, showing a high level of sequence conservation. B. Sequence of the wild type and mutant type of MO25. C. The relationship between miR-429 and MO25 was analyzed by dual luciferase reporter assay. D. After miR-429 mimic or antagomiR-429 was transfected into cardiomyocytes, the level of miR-429 was measured by Real-time PCR. E. The expression of MO25 was measured by Western blotting in miR-429 manipulated cardiomyocytes under normal and AR condition. $^{*}P < 0.05$.

also found that the expression of p62 and LC3B-I/II was dramatically increased in 2 and 4 weeks of MI mouse (Fig. 1B, $P < 0.05$). In addition, when the cultured neonatal rat cardiomyocytes were exposed to different time of anoxia, the expression of miR-429 was noticeably decreased (Fig. 1C, $P < 0.05$), and the expression of p62 and LC3BI/II was dramatically increased (Fig. 1D, $P < 0.05$). As an identified regulator of autophagy, the expression of MO25 was also significantly upregulated in IR mice and A/R treated cardiomyocytes (Fig. 1B and D, $P < 0.05$). These results may suggest that miR-429 was associated with autophagy.

3.2. MO25 was the direct target gene of miR-429

The TargetScan 7.0 software showed that MO25 was the target of mmu-miR-429: MO25 was conserved in various mammals (including rat, chimp, rhesus, mouse, et al.) with the target sequence of CAGUAUU (Fig. 2A). Next, the dual luciferase activity assay was conducted to further confirm the relationship between miR-429 and MO25. The wild and mutant type of MO25 sequences were shown as Fig. 2B. The results of dual luciferase activity assay showed that when cells were co-transfected with miR-429 mimic and MO25-WT, the luciferase activity was dramatically decreased (Fig. 2C, $P < 0.05$). Moreover, we evaluated the possibility that p62 and/or LC3B were also targets genes of miR-429. Our data showed that there were no potential targeting sites of miR-429 on 3′UTRs of p62 nor LC3B (Fig. S1A and B), and the luciferase reporter assay also showed that miR-429 mimic could not decreased the luciferase activity of psi-p62 nor psi-LC3B (Fig. S1C), indicating that p62 and LC3B were not target genes of miR-429. Finally, we analyzed the effect of miR-429 on the expression of MO25. The results showed that when the cultured neonatal rat cardiomyocytes were transfected with miR-429 mimic, the expression of miR-429 was significantly increased, and antagomiR-429 dramatically reduced miR-429 expression (Fig. 2D, $P < 0.05$). Furthermore, with or without the treatment of AR, when miR-429 mimic was transfected into the cells, the expression of MO25 was dramatically decreased, and antagomiR-429 increased the MO25 expression (Fig. 2E).

3.3. AntagomiR-429 enhanced autophagy and suppressed apoptosis in cardiomyocytes, and miR-429 mimic showed the opposite effects

The further study was performed to analyze whether miR-429 played a role in autophagy. The results showed that antagomiR-429 significantly increased the percentage of GFP-LC3B labelled cardiomyocytes, increased the number of autophagy vesicles and autophagosomes both under normal condition and AR treatment (Fig. 3A, B, C; $P < 0.05$). AntagomiR-429 dramatically decreased the cell apoptosis (Fig. 3D, $P < 0.05$). Whereas miR-429 mimic only noticeably decreased the percentage of GFP-LC3B labelled cardiomyocytes, reduced the number of autophagy vesicles and autophagosomes in the condition of AR treatment (Fig. 3A–C; $P < 0.05$). Furthermore, miR-429 mimic significantly increased the cell apoptosis both in the condition of normal and AR treatment (Fig. 3D, $P < 0.05$). Western blotting showed that the expression of MO25, LKB1, ATG13, p62 LC3B-II/LC3B-I and activation of AMPKa (manifested by the proportion of pAMPKa/AMPKa), was suppressed dramatically by miR-429 mimic; whereas they were noticeably up-regulated by antagomiR-429 (Fig. 3E, $P < 0.05$). These results indicated that inhibition of miR-429 enhanced the autophagy and suppressed apoptosis.

3.4. Inhibition of MO25 expression by MO25-siRNA transfection rescued the effect of antagomiR-429 on autophagy and apoptosis in A/R-treated cardiomyocytes

Furthermore, to confirm that MO25 mediated the effect of miR-429 on cardiomyocyte autophagy, a specific siRNA against MO25 was applied in cell transfection experiments under A/R condition. The results showed that MO25 siRNA decreased the percentage of GFP-LC3B labelled cardiomyocytes, reduced the number of autophagy vesicles and autophagosomes, and promoted cell apoptosis, which displayed an opposite effect to that of antagomir-429 (Fig. 4A–D). In consistent with the changes in cell behaviors, MO25 siRNA inhibited the expression of MO25, LKB1 and the autophagy marker genes, and suppressed activation of AMPKα (Fig. 4E). Moreover, MO25 siRNA rescued the effect of antagomiR-429 on autophagy, apoptosis and gene expression in A/R-treated cardiomyocytes (Fig. 4A–E).

3.5. Inhibition of miR-429 reduced myocardial infarct size in mouse

Finally, to verify the effect of miR-429 on IR injury *in vivo*, the antagomiR-429 was injected into the left ventricular myocardium of mouse. The results showed that when the mouse in sham group or I/R group were injected with antagomiR-429, the expression of antagomiR-429 was dramatically down-regulated compared with control anta group (Fig. 5A). In addition, antagomiR-429 significantly increased the weight of left ventricular (LVw) and the ratio of LVw/body weight (BW), and reduced the infarct size (Fig. 5B–D; $P < 0.05$). Echocardiography analysis showed that antagomiR-429 improved the maximum rate of increase of left ventricular pressure (+dp/dt max) and left ventricular end-diastolic pressure (LVEDP) in I/R mice (Fig. 5E and F), suggesting that inhibition of miR-429 might improve the systolic function and the diastolic function of left ventricle. Furthermore, we also found that antagomiR-429 significantly increased the expression of MO25, LKB1 and the autophagy marker genes and activation of AMPKa (Fig. 5G, $P < 0.05$). These results indicate that antagomiR-429 played a protect role in IR mice.

4. Discussion

Increasing studies have proved that miRNAs play a vital role in the progression of MI. For example, miR-199b-5p participated in post-infract remodeling by simultaneous regulation of Dyrk1a, notch 1 receptor and its ligand jagged1 [17]; miR-208b and miR-34a was reported to be dramatically up-regulated in patients with remodeling and associated with increased risk of mortality or heart failure [18]. Our results proved that miR-429 was significantly down-regulated in IR mouse and AR treated cells. It is interesting that this result is contradictory to the reports by other groups, which showed increased miR-429 after hypoxia exposure in culture cardiomyocytes and endothelial cells. After retrieving and reading the literature on miR-429, we found it is very interesting that, in the same tissue subjected to adverse stimuli (including hypoxia, drugs and radiation), miR-429 unexpectedly displayed showed different expression patterns or functioned differently. For example, in brain damaged by hypoxia-ischemia, miR-429 was downregulated, negatively regulated apoptosis and protected brain neurons against hypoxic-ischemic damage [19], while, in Aβ-induced brain damage, miR-429 was upregulated, promoted apoptosis and contributed to Aβ-induced damage of brain neurons [20]. Another example is that, in angiotensin II-induced injury of kidney, miR-429 was downregulated and contributed to renal fibrosis [21], whereas, in acute injured kidney, miR-429 also promoted renal fibrosis, but its expression was upregulated [22]. Moreover, it was indeed that miR-429 expression was shown to be upregulated by hypoxia in cardiomyocytes and vascular endothelial cells, but a previous study showed that miR-429 expression was significantly upregulated by aerobic exercise training [23]. Therefore, it is really hard to determine the expression pattern and function of miR-429 during a relatively short or static process.

Autophagy is a lysosomal degradation pathway that is essential for survival, differentiation, development, and homeostasis [24]. Autophagy was considered as a vital regulator of IR injury and played an important role in the heart during ischemia and reperfusion [25]. It is reported that the up-regulation of autophagy in the failing hearts protected cardiomyocytes from pressure overload. Our results showed that antagomiR-429 significantly increased the number of GFP-LC3B

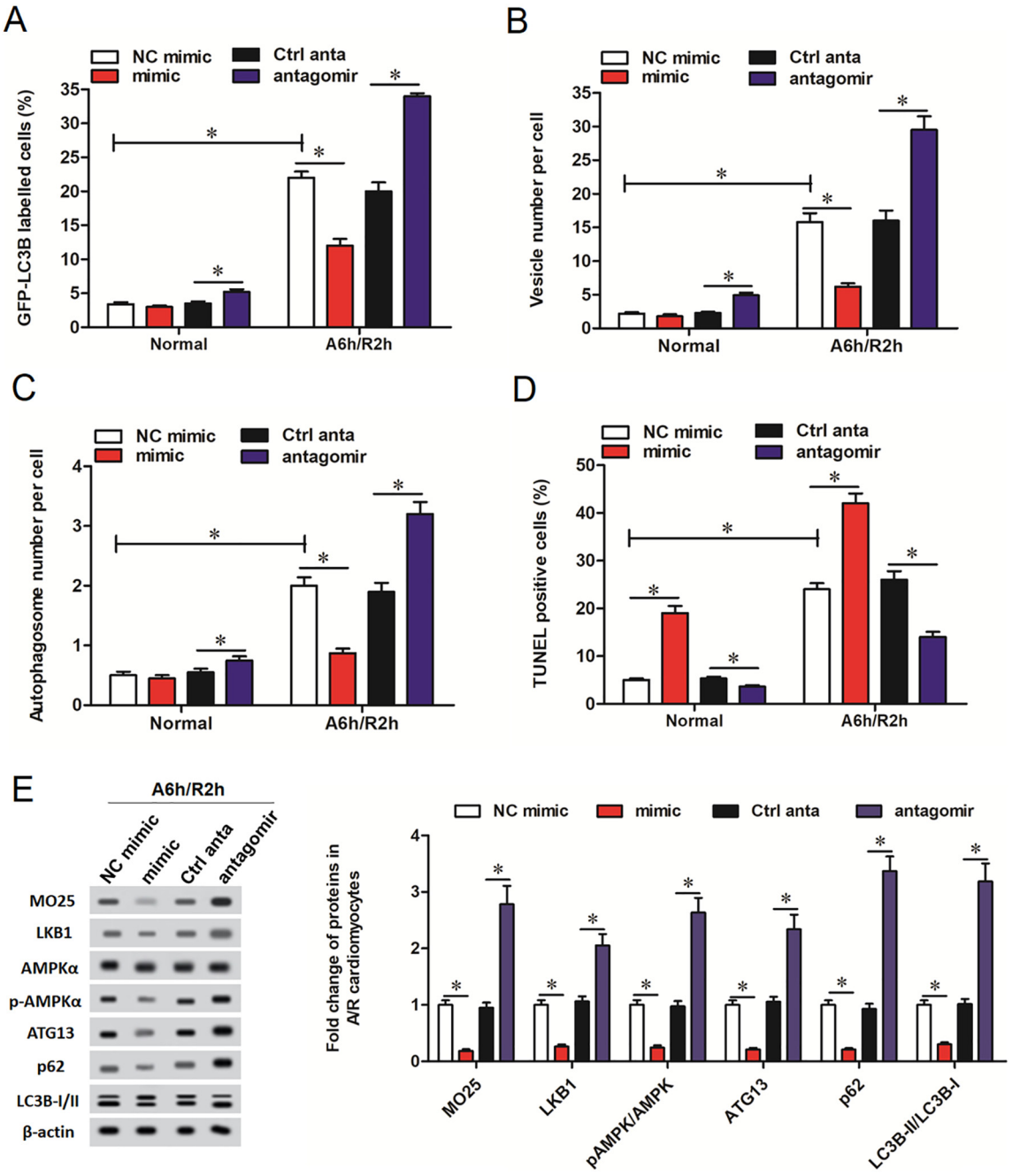

Fig. 3. AntagomiR-429 enhanced the autophagy and suppressed apoptosis, whereas miR-429 mimic showed the opposite effect. A. After cardiomyocytes were treated with miR-429 mimic (40 nM), antagomiR-429 (60 nM) or their relative controls, and cells were treated with A6h/R2h, the percentage of cells that labelled with GFP-LC3 was quantified. B. The vesicle number in each cardiomyocyte was determined. C. The number of autophagosomes in each cardiomyocyte was determined by electron microscopy. D. Cell apoptosis was measured by the TUNEL method. E. The expression of MO25, LKB1, pAMPKa, AMPKa, ATG13, p62 and LC3BI/II was measured by Western blotting. *$P < 0.05$.

labelled cells, increased the number of vesicle and autophagosome, and decreased the cell apoptosis both under the normal and AR condition. Furthermore, antagomiR-429 reduced myocardial infarct size in I/R mice. In conclusion, these may indicate that antagomiR-429 ameliorates AR injury in cardiomyocytes by enhancing autophagy.

Adenosine monophosphate-activated protein kinase (AMPK) acted as a principal intracellular energy sensor and involved in the induction of autophagy [26]. Previous study also proved that AMPK mediated autophagy during myocardial ischemia *in vivo* [27]. Furthermore, the activity of AMPK was regulated by upstream LKB1 at Thr-172 (α subunit) phosphorylation. As a member of LKB1 complex, MO25 was required for full LKB1 activity [28]. In the present study, our results showed that MO25 was the direct target gene of miR-429. Inhibition of miR-429 expression dramatically increased the expression of MO25. When the primary cultured cardiomyocytes were treated with AR, the expression of MO25, LKB1, pAMPKα, ATG13, p62 and LC3B-I/II were increased in antagomiR-429 transfection group. Moreover, the *in vivo* study also showed that antagomiR-429 dramatically increased the expression of MO25, LKB1, pAMPKα, ATG13, p62 and LC3B-I/II. These results confirmed that antagomiR-429 ameliorates AR injury in cardiomyocytes by enhancing autophagy through activated the MO25/LKB1/AMPK pathway.

In conclusion, the presented study proved that antagomiR-429 ameliorates AR injury in cardiomyocytes by enhancing MO25/LKB1/

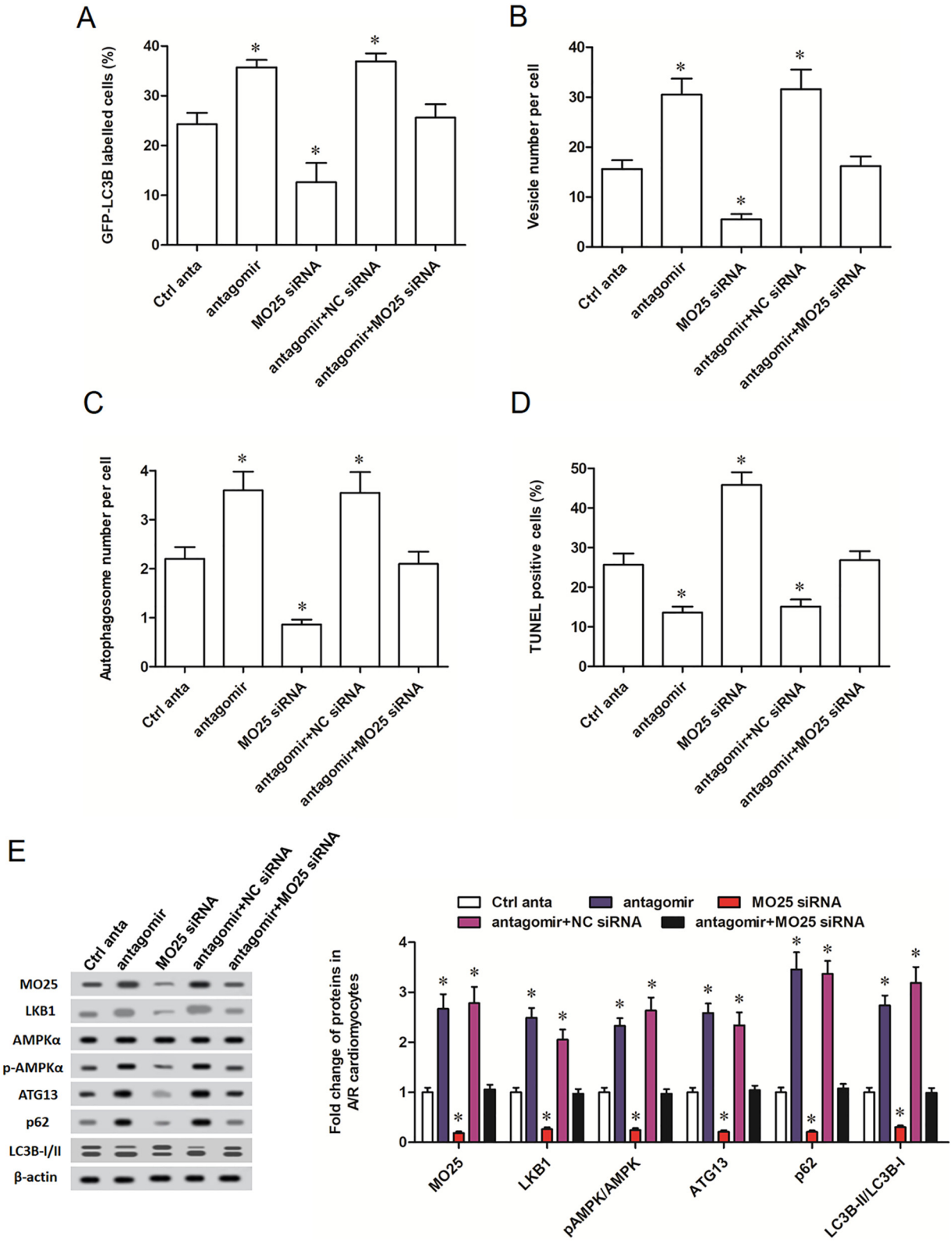

Fig. 4. Inhibition of MO25 reduced the effect of antagomir-429 on autophagy and apoptosis in AR cardiomyocytes. Cardiomyocytes were treated with control antagomir (40 nM), antagomir-429 (40 nM), MO25 siRNA (50 nM), 40 nM antagomir-429 + 50 nM NC siRNA, and 40 nM antagomir-429 + 50 nM MO25 siRNA. After incubation for 48 h, the cardiomyocytes were treated with A6h/R2h. A. The percentage of cells that labelled with GFP-LC3 was quantified. B. The vesicle number in each cardiomyocyte was determined. C. The number of autophagosomes in each cardiomyocyte was determined by electron microscopy. D. Cell apoptosis was measured by the TUNEL method. E. The expression of MO25, LKB1, pAMPKa, AMPKa, ATG13, p62 and LC3BI/II was measured by Western blotting. *$P < 0.05$ *vs* ctrl anta group.

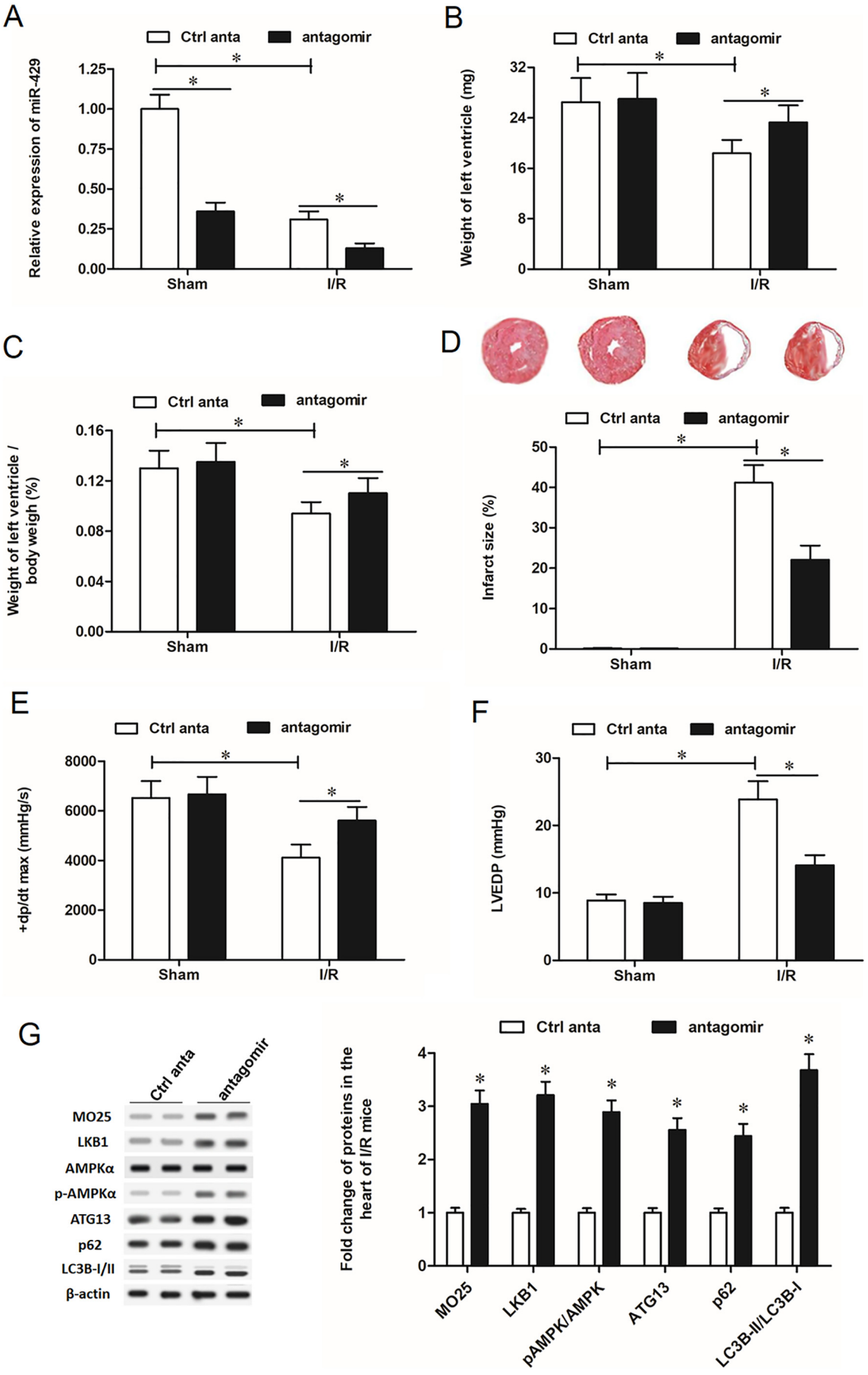

(caption on next page)

Fig. 5. Inhibition of miR-429 reduced myocardial infarct size in mice. Sham treated mice or I/R mice were administrated with Ctrl-antagomir or antagomiR-429. At the end of week 4, A. the expression of miR-429 was measured by Real-time PCR. B. The weight of left ventricle was measured. C. The proportion of weight of left ventricle occupied in body weight was calculated. D. The infarct size was measured by TTC staining and expressed as percentage of total left ventricular. The values of (E) + dp/dt max and (F) LVEDP were detected with echocardiography analysis by using the BL-420S Biology Function Laboratory System. G. The expression of MO25, LKB1, pAMPKa, AMPKa, ATG13, p62 and LC3BI/II was measured by Western blotting. $^{*}P < 0.05$ *vs* ctrl anta group.

AMPK mediated autophagy. MiR-429 may be a potential novel therapeutic target for myocardial IR injury.

Supplementary data to this article can be found online at https://doi.org/10.1016/j.lfs.2019.116842.

Declaration of competing interest

The authors declare that there are no conflicts of interest.

References

[1] H.D. White, K. Thygesen, J.S. Alpert, A.S. Jaffe, Republished: clinical implications of the third universal definition of myocardial infarction, Heart 100 (2014) 424–432.

[2] Z. Liu, D. Yang, P. Xie, G. Ren, G. Sun, X. Zeng, X. Sun, MiR-106b and MiR-15b modulate apoptosis and angiogenesis in myocardial infarction, Cell. Physiol. Biochem. 29 (2012) 851–862.

[3] P. Liu, C. Qiu, B. Li, X. Ding, Z. Wang, Y. Li, Y. Dang, Y. Liu, W. Li, T. Hu, Clinical impact of circulating miR-133, miR-1291 and miR-663b in plasma of patients with acute myocardial infarction, Diagn. Pathol. 9 (2014) 1–7.

[4] A. Moran, D. Gu, D. Zhao, P. Coxson, Y.C. Wang, C.S. Chen, J. Liu, J. Cheng, K. Bibbinsdomingo, Y.M. Shen, Future cardiovascular disease in China Markov model and risk factor scenario projections from the coronary heart disease policy model–China, Circ. Cardiovasc. Qual. Outcomes 3 (2010) 243–252.

[5] L. Liu, G. Zhang, Z. Liang, X. Liu, T. Li, J. Fan, J. Bai, Y. Wang, MicroRNA-15b enhances hypoxia/reoxygenation-induced apoptosis of cardiomyocytes via a mitochondrial apoptotic pathway, Apoptosis 19 (2014) 19–29.

[6] L. Zhang, X. Chen, T. Su, H. Li, Q. Huang, D. Wu, C. Yang, Z. Han, Circulating miR-499 are novel and sensitive biomarker of acute myocardial infarction, J. Thorac. Dis. 7 (2015) 303–308.

[7] M. Xu, G. Meng, Z. Ke, J. Zhou, W. Zhong, J. Da, miR-203 inhibition of renal cancer cell proliferation, migration and invasion by targeting of FGF2, Diagn. Pathol. 10 (2015) 1–9.

[8] L. Wang, L. Li, R. Guo, X. Li, Y. Lu, X. Guan, S.C. Gitau, C. Xu, B. Yang, miR-101 promotes breast cancer cell apoptosis by targeting Janus kinase 2, Cell. Physiol. Biochem. 34 (2014) 413–422.

[9] T. Umezu, H. Tadokoro, K. Azuma, S. Yoshizawa, K. Ohyashiki, J.H. Ohyashiki, Exosomal miR-135b shed from hypoxic multiple myeloma cells enhances angiogenesis by targeting factor-inhibiting HIF-1, Blood 124 (2014) 3748–3757.

[10] K. Liu, J. Huang, M. Xie, Y. Yu, S. Zhu, R. Kang, L. Cao, D. Tang, X. Duan, MIR34A regulates autophagy and apoptosis by targeting HMGB1 in the retinoblastoma cell, Autophagy 10 (2014) 442–452.

[11] E. Coskunpinar, H.A. Cakmak, A.K. Kalkan, N.O. Tiryakioglu, M. Erturk, Z. Ongen, Circulating miR-221-3p as a novel marker for early prediction of acute myocardial infarction, Gene 591 (2016) 90–96.

[12] J. Zhu, K. Yao, Q. Wang, J. Guo, H. Shi, L. Ma, H. Liu, W. Gao, Y. Zou, J. Ge, Circulating miR-181a as a potential novel biomarker for diagnosis of acute myocardial infarction, Cell. Physiol. Biochem. 40 (2016) 1591–1602.

[13] L. Huang, L. Li, X. Chen, H. Zhang, Z. Shi, MiR-103a targeting Piezo1 is involved in acute myocardial infarction through regulating endothelium function, Cardiol. J. (2016) 556–562.

[14] H. Xu, L. Jin, Y. Chen, J. Li, Downregulation of microRNA-429 protects cardiomyocytes against hypoxia-induced apoptosis by increasing Notch1 expression, Int. J. Mol. Med. 37 (2016) 1677–1685.

[15] Y. Yan, Y. Liao, L. Yang, J. Wu, J. Du, W. Xuan, L. Ji, Q. Huang, Y. Liu, J. Bin, Late-phase detection of recent myocardial ischaemia using ultrasound molecular imaging targeted to intercellular adhesion molecule-1, Cardiovasc. Res. 89 (2011) 175–183.

[16] X.H. Liao, N. Wang, Q.X. Liu, T. Qin, B. Cao, D.S. Cao, T.C. Zhang, Myocardin-related transcription factor-a induces cardiomyocyte hypertrophy, IUBMB Life 63 (2011) 54–61.

[17] B. Duygu, E.M. Poels, R. Juni, N. Bitsch, L. Ottaviani, S. Olieslagers, L.J.d. Windt, P.A.d.C. Martins, miR-199b-5p is a regulator of left ventricular remodeling following myocardial infarction, Res. 2 (2017) 18–26.

[18] P. Lv, M. Zhou, J. He, W. Meng, X. Ma, S. Dong, X. Meng, X. Zhao, X. Wang, F. He, Circulating miR-208b and miR-34a are associated with left ventricular remodeling after acute myocardial infarction, Int. J. Mol. Sci. 15 (2014) 5774–5788.

[19] H. Fang, H.F. Li, M.H. He, J.Y. Yan, M. Yang, F.X. Zhang, R.R. Wang, Q.Y. Wang, J.P. Zhang, Long non-coding RNA MALAT1 sponges microRNA-429 to regulate apoptosis of hippocampal neurons in hypoxic-ischemic brain damage by regulating WNT1, Brain Res. Bull. 8 (2019) 1–10.

[20] S. Fu, J. Zhang, S. Zhang, Knockdown of miR-429 attenuates Abeta-induced neuronal damage by targeting SOX2 and BCL2 in mouse cortical neurons, Neurochem. Res. 43 (2018) 2240–2251.

[21] Z. Wang, Q. Zhu, W. Wang, J. Hu, P.L. Li, F. Yi, N. Li, Downregulation of microRNA-429 contributes to angiotensin II-induced profibrotic effect in rat kidney, Am. J. Physiol. Renal. Physiol. 315 (2018) F1536–F1541.

[22] H. Sonoda, B.R. Lee, K.H. Park, D. Nihalani, J.H. Yoon, M. Ikeda, S.H. Kwon, miRNA profiling of urinary exosomes to assess the progression of acute kidney injury, Sci. Rep. 9 (2019) 4692–4702.

[23] R.W. Souza, G.J. Fernandez, J.P. Cunha, W.P. Piedade, L.C. Soares, P.A. Souza, D.H. de Campos, K. Okoshi, A.C. Cicogna, M. Dal-Pai-Silva, R.F. Carvalho, Regulation of cardiac microRNAs induced by aerobic exercise training during heart failure, Am. J. Physiol. Heart Circ. Physiol. 309 (2015) H1629–H1641.

[24] B. Levine, Autophagy in the pathogenesis of disease, Cell 132 (2008) 27–42.

[25] X. Wu, L. He, F. Chen, X. He, Y. Cai, G. Zhang, Q. Yi, M. He, J. Luo, Impaired autophagy contributes to adverse cardiac remodeling in acute myocardial infarction, PLoS One 9 (2014) e112891.

[26] L. Harhaji-Trajkovic, U. Vilimanovich, T. Kravic-Stevovic, V. Bumbasirevic, V. Trajkovic, AMPK-mediated autophagy inhibits apoptosis in cisplatin-treated tumour cells, J. Cell. Mol. Med. 13 (2009) 3644–3654.

[27] H. Takagi, Y. Matsui, S. Hirotani, H. Sakoda, T. Asano, J. Sadoshima, AMPK mediates autophagy during myocardial ischemia in vivo, Autophagy 3 (2007) 405.

[28] H. Chen, G.M. Untiveros, L.A. Mckee, J. Perez, J. Li, P.B. Antin, J.P. Konhilas, Micro-RNA-195 and -451 regulate the LKB1/AMPK signaling axis by targeting MO25, PLoS One 7 (2012) e41574.